

# A Systematic Evaluation of Positional Bias in Multi-Video Summarization with MLLMs

Huangchen Xu<sup>1</sup>, Yuan Wu<sup>1,\*</sup>, Yi Chang<sup>1,2,3,\*</sup>

<sup>1</sup>School of Artificial Intelligence, Jilin University

<sup>2</sup>Engineering Research Center of Knowledge-Driven Human-Machine Intelligence, Jilin University

<sup>3</sup>International Center of Future Science, Jilin University

xuhc9924@mails.jlu.edu.cn, yuanwu@jlu.edu.cn, yichang@jlu.edu.cn

## Abstract

Multimodal Large Language Models (MLLMs) are increasingly used for video understanding, yet their reliability under multi-video inputs remains poorly understood. We study positional bias in multi-video summarization, where the quality of a per-video summary can change with the video’s input slot even when the underlying content is unchanged. We construct a benchmark from ActivityNet and News videos, covering Cooking, Domestic, Leisure, and News settings with two- and four-video inputs. We evaluate nine open-source and proprietary MLLMs and measure position effects with three complementary metrics: Coverage, Directional Positional Bias (DPB), and Middle-Edge Gap (MEG). Our results show that positional effects are domain- and model-dependent: signed directional bias can be small even when middle positions underperform, and increasing visual or generation budget does not uniformly remove the imbalance. We further analyze prompt-level mitigation methods. Together, the results show that multi-video summarization remains sensitive to input protocol and position, motivating more robust order-invariant multimodal systems.

## 1 Introduction

Video summarization aims to condense video content into shorter yet informative representations while preserving essential information and temporal coherence (Kansal et al., 2023). As Multimodal Large Language Models (MLLMs) become increasingly capable of processing video inputs, they have become a promising foundation for open-ended video summarization. Recent benchmarks have evaluated MLLMs on long-video understanding (Zhou et al., 2025) and video summarization (Jung and Kim, 2025). Meanwhile, emerging *multi-video* benchmarks have shifted attention to inputs containing multiple videos, but they primarily target understanding, perception, or reasoning

rather than summarization (Peng et al., 2025; Bai et al., 2026). Less is known about *multi-video summarization*, where the model must generate one aligned summary for each video in the same input.

A key concern is *positional bias*, where model performance changes with input order rather than the underlying content. In NLP, large language models have been shown to favor early content in news summarization (Grenander et al., 2019) and to exhibit “lost in the middle” behavior in long-context settings (Liu et al., 2024). Recent multimodal work has also examined positional effects in multi-image understanding (Tian et al., 2025) and video probing benchmarks (Xia et al., 2025). Yet these protocols mainly test whether models can retrieve or use target evidence after its position changes. Multi-video summarization poses a different challenge: the model must bind each summary to the correct video while balancing limited summary detail across multiple input slots.

In this work, we present a systematic study of positional bias in multi-video summarization. We construct a benchmark from ActivityNet (Heilbron et al., 2015) and the News Video Dataset (Whitehead et al., 2018), covering four scenario categories: *Cooking*, *Domestic*, *Leisure*, and *News*. We evaluate both pairwise and four-video inputs using cyclic orderings, so that each video appears at each position exactly once. Because lexical-overlap metrics are insufficient for this highly abstractive task, we use dataset-adaptive and reference-based Coverage: ActivityNet-derived domains are scored with an LLM-as-a-Judge protocol, while News uses extractive reference-fragment coverage. We then report Coverage, Directional Positional Bias (DPB), and Middle-Edge Gap (MEG) to distinguish overall information preservation, earlier-versus-later preference, and middle-position weakness. Anonymous code and data are available at <https://anonymous.4open.science/r/annoym07>.

Our contributions are as follows:

1. **Benchmark and evaluation protocol:** We construct a benchmark over *Cooking*, *Domestic*, *Leisure*, and *News*. We also introduce an evaluation protocol that measures Coverage, Directional Positional Bias (DPB), and Middle-Edge Gap (MEG), separating earlier-versus-later preference from middle-position weakness.
2. **Model- and domain-dependent positional effects:** We evaluate nine open-source and proprietary MLLMs and show that positional effects are model- and domain-dependent. Several settings have near-zero DPB but negative MEG, which would be missed by directional bias alone.
3. **Robustness checks and mitigation analysis:** We examine visual budget, requested summary length, boundary format, prompt placement, and mitigation to analyze position effects.

## 2 Related Work

### 2.1 Positional Bias

Positional bias refers to models’ sensitivity to where information or candidates appear in the input, beyond their underlying content. In text settings, prior work has studied lead or position bias in summarization (Grenander et al., 2019; Schilcher et al., 2025), the “lost in the middle” effect in long-context QA and retrieval (Liu et al., 2024), and position-dependent faithfulness in long-form summarization (Wan et al., 2025). Similar order effects also appear when LLMs are used as judges, rankers, or recommenders (Wang et al., 2024; Shi et al., 2025; Koo et al., 2024; Hou et al., 2024). These studies motivate a range of mitigation strategies, from training or attention-based methods to lightweight inference-time controls such as order perturbation and attention-guiding prompts (Wang et al., 2024; Zhang et al., 2024; Wan et al., 2025; Tian et al., 2025).

In multimodal settings, recent work has begun to identify analogous effects. Tian et al. (2025) show that reordering images can substantially affect multi-image reasoning, while Video-LevelGauge (Xia et al., 2025) studies video LLMs through probing tasks that place relevant visual evidence at different positions. Our work differs in both task structure and evaluation target. Rather than testing whether a model retrieves localized

evidence from a moved probe, we study whether it maintains balanced information coverage when generating aligned summaries for multiple videos under different input orders.

### 2.2 Automatic Evaluation for Summarization

Automatic summarization evaluation has long relied on lexical-overlap metrics such as BLEU, ROUGE, and METEOR (Chang et al., 2024; Papineni et al., 2002; Lin, 2004; Banerjee and Lavie, 2005), and later embedding-based metrics such as BERTScore (Zhang et al., 2020). These metrics are inexpensive and scalable, but they mainly measure text similarity and do not directly assess whether the generated summary preserves or aligns with specific information in the reference.

Recent work has explored more semantic evaluation protocols. LLM-based evaluators such as GPTScore and G-Eval use large language models to judge generated text along flexible task-specific criteria (Fu et al., 2024; Liu et al., 2023). QA-based metrics such as QuestEval evaluate summarization through question generation and question answering (Rebuffel et al., 2021), and recent video-summary evaluation further uses multimodal QA to assess coverage, factuality, and chronology (Jung and Kim, 2025). These approaches provide richer diagnostics than surface overlap, but they can require multiple model calls per summary and are costly for large-scale position-wise evaluation over many videos, orders, and slots.

For short news summaries, extractive-fragment analysis provides another useful perspective by measuring partial phrase-level overlap (Grusky et al., 2018). This line of work is especially relevant when references are concise and contain fixed named entities or event phrases.

## 3 Evaluation

Figure 1 illustrates our evaluation pipeline. We construct multi-video inputs, prompt the model to generate aligned per-video summaries, and evaluate positional effects with cyclic orderings across multiple settings, including model families, domains, video durations, and visual-budget variants. We then quantify positional effects using three metrics: *Coverage*, *Directional Positional Bias* (DPB), and *Middle-Edge Gap* (MEG).

### 3.1 Data Collection

We build our benchmark from two public datasets with human-written reference summaries, cover-

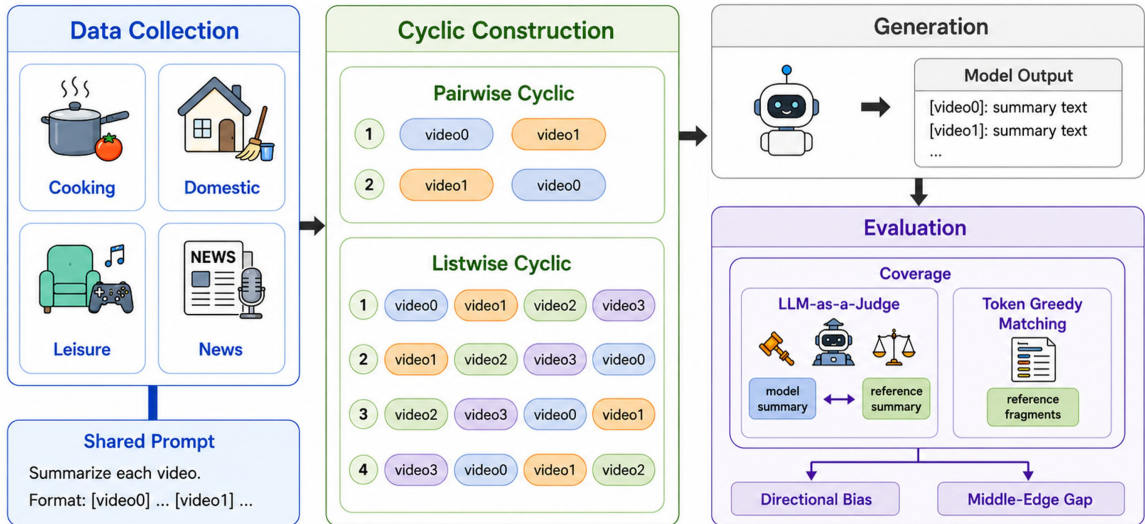


Figure 1: Overview of our evaluation pipeline. We construct cyclic orderings for pairwise and listwise multi-video inputs, generate aligned per-video summaries, and evaluate positional effects with three complementary metrics.

ing four scenario categories: *Cooking*, *Domestic*, *Leisure*, and *News*. For *News*, we use the News Video Dataset (Whitehead et al., 2018). For the other three categories, we sample from ActivityNet (Heilbron et al., 2015): *Cooking* corresponds to eating and cooking activities, *Domestic* to household activities, and *Leisure* to social, relaxation, and recreational activities.

These categories instantiate common online video-use settings. Prior work shows that users often encounter streams or sets of videos through recommendation-driven multi-video browsing, use online video platforms for how-to learning, leisure viewing, and current events, and increasingly consume news through social platforms (Smith et al., 2018; Covington et al., 2016).

To study the interaction between positional effects and video duration, we partition inputs into short videos (0–1 minute) and longer-duration videos (1–2 minutes). *Cooking* and *News* contain only short-video settings, while *Domestic* and *Leisure* contain both short- and longer-duration settings. For each domain–duration configuration, we randomly sample 27 video groups. The four-video groups are non-overlapping within each topic–duration configuration, while the pairwise and four-video settings may share videos within the same topic. This yields 708 unique videos in total. Although the number of unique videos is limited, cyclic-based evaluation produces thousands of order-controlled instances, enabling systematic analysis under a manageable inference budget.

### 3.2 Summary Generation and Alignment

**Models.** We evaluate both proprietary and open-source MLLMs. The main comparison includes InternVL3.5-8B, InternVL3.5-14B (Wang et al., 2025), Qwen3-VL-8B, Qwen3-VL-30B-A3B (Bai et al., 2025), MiniCPM-o-4.5 (Cui et al., 2026), GLM-4.1V-9B-Thinking (Team et al., 2026), MiMo-VL-7B-RL (Xiaomi, 2025), Gemini-3.1-Pro (Google DeepMind, 2026), and GPT-5.4 (OpenAI, 2026).

**Input scale.** We focus on two input scales: pairwise inputs with two videos ( $P=2$ ) and listwise inputs with four videos ( $P=4$ ). For each scale, we use a cyclic permutation design so that each video appears at every position exactly once. This supports balanced within-video positional analysis while keeping the number of permutations tractable. We use domain-scale notation (e.g., *Cooking-2*, *News-4*) to denote experiments on a specific domain with a given number of input videos.

**Input configuration.** All main runs use the same task protocol: the task instruction and output format are given first, followed by labeled video clips in cyclic order, with a blank boundary frame between consecutive clips. We use  $\text{top}_p=1.0$  and temperature 0.9 unless otherwise specified.

We set the requested summary length according to reference granularity: ActivityNet-derived references average about 3.4 sentences per video, so we ask for four sentences per video; News references average about 1.2 sentences, so we ask for two sentences per video. For frame-based in-

puts, we uniformly sample frames, using 16 frames per video for short-video and 24 frames for longer ActivityNet settings when supported. The default resolution is  $448 \times 448$ .

**Per-video summary alignment.** We use a two-stage alignment strategy. First, we instruct the model to produce per-video summaries with a fixed template such as [video0] . . . , [video1] . . . , and extract the segments by pattern matching. When the output deviates from the template, we apply a fallback semantic alignment: we split the reference summaries and model output into sentences, compute sentence-level semantic similarity, and assign each generated sentence to the video with the highest similarity score. Sentences assigned to the same video are then concatenated into the aligned per-video summary.

### 3.3 Evaluation Metrics

Let  $P$  be the number of input videos and  $p \in \{1, \dots, P\}$  the slot position. We denote the coverage score of the video at position  $p$  in instance  $i$  by  $C_{i,p}$ .

#### 3.3.1 Coverage.

Coverage measures whether the generated summary preserves the key information in the human-written reference. Because reference granularity differs across datasets, we use dataset-adaptive estimators.

For ActivityNet-based domains, we use sentence-level semantic coverage. Given reference sentences and the generated summary for the same video, GPT-5.1 (OpenAI, 2025) judges whether each reference sentence is covered, allowing paraphrases and minor wording differences. Let  $N_{\text{cov}}^{(i,p)}$  be the number of covered reference sentences and  $N_{\text{ref}}^{(i,p)}$  the total number of reference sentences:

$$C_{i,p} = \frac{N_{\text{cov}}^{(i,p)}}{N_{\text{ref}}^{(i,p)}}. \quad (1)$$

For News, references are much shorter, averaging about 1.2 sentences per video, and their key information often lies in specific named entities, locations, organizations, and event phrases. Binary sentence-level scoring is therefore too coarse: it can miss partial preservation of these surface-specific details. We instead use reference-fragment coverage inspired by NEWSROOM (Grusky et al., 2018): we greedily match the longest contiguous reference spans appearing in the generated sum-

mary and compute the proportion of matched reference tokens:

$$C_{i,p}^{\text{frag}} = \frac{|\mathcal{M}_{i,p}|}{|r_{i,p}|}, \quad (2)$$

where  $\mathcal{M}_{i,p}$  is the set of matched reference-token positions and  $|r_{i,p}|$  is the number of reference tokens.

#### 3.3.2 Directional Positional Bias.

Directional Positional Bias (DPB) measures earlier-versus-later preference. We assign each position a linear weight

$$\alpha_p = \frac{2p - P - 1}{P - 1}, \quad (3)$$

where  $\alpha_1 = -1$  and  $\alpha_P = 1$ . For instance  $i$ :

$$\text{DPB}_i = \frac{\sum_{p=1}^P \alpha_p C_{i,p}}{\sum_{p=1}^P C_{i,p} + \epsilon}, \quad (4)$$

and aggregate over instances:

$$\text{DPB} = \frac{1}{N} \sum_{i=1}^N \text{DPB}_i. \quad (5)$$

Negative values indicate earlier-position preference, and positive values indicate later-position preference. Near-zero DPB does not imply position invariance, since non-monotonic effects, such as middle-position weakness, can cancel out in this signed measure. We therefore also use Middle-Edge Gap (MEG) to capture whether middle positions underperform edge positions in four-video inputs.

#### 3.3.3 Middle-Edge Gap.

For four-video inputs ( $P = 4$ ), we define MEG as:

$$\text{MEG}_i = \frac{C_{i,2} + C_{i,3}}{2} - \frac{C_{i,1} + C_{i,4}}{2}, \quad (6)$$

with aggregate

$$\text{MEG} = \frac{1}{N} \sum_{i=1}^N \text{MEG}_i. \quad (7)$$

Negative MEG indicates middle-position weakness, while positive MEG indicates a middle-position advantage.

## 4 Experimental Results

### 4.1 Main Results

Table 1 shows that positional effects do not reduce to a single universal primacy or recency pattern. Instead, the dominant pattern is heterogeneity across models and domains.

Model	Duration	Cooking-2		Cooking-4		Domestic-2		Domestic-4		Leisure-2		Leisure-4		News-2		News-4	
		DPB (%)	MEG (%)	DPB (%)	MEG (%)	DPB (%)	MEG (%)	DPB (%)	MEG (%)	DPB (%)	MEG (%)	DPB (%)	MEG (%)	DPB (%)	MEG (%)	DPB (%)	MEG (%)
Qwen3-VL-8B	Short	-3.33	-2.67	-1.34	8.13	-0.37	-2.57	6.01	0.67	-0.64	0.94	1.17	0.15				
Qwen3-VL-8B	Long	-	-	-	-5.24	-2.90	-2.45	0.71	-2.37	-0.71	-	-	-	-	-	-	-
InternVL3.5-8B	Short	-3.34	-4.16	-3.34	-3.27	1.67	-4.50	-0.15	-2.07	-0.10	1.67	-0.99	-1.04				
InternVL3.5-8B	Long	-	-	-	2.27	-0.94	-3.34	13.89	-1.28	-0.57	-	-	-	-	-	-	-
InternVL3.5-14B	Short	-5.93	-1.74	0.40	4.06	-2.51	-2.11	-3.04	0.07	-2.65	1.61	0.92	-1.49				
InternVL3.5-14B	Long	-	-	-	-4.96	-0.98	-3.15	-8.35	-0.77	-1.41	-	-	-	-	-	-	-
Qwen3-VL-30B-A3B	Short	-5.68	-1.41	2.41	0.42	3.26	-2.63	9.36	-0.08	-0.76	2.11	0.09	-0.51				
Qwen3-VL-30B-A3B	Long	-	-	-	5.01	-0.89	-3.68	-2.96	1.50	-1.23	-	-	-	-	-	-	-
MiniCPM-o-4.5	Short	-1.44	-1.56	-0.51	-2.69	1.56	1.92	3.06	1.82	0.21	-1.31	-0.50	-1.00				
MiniCPM-o-4.5	Long	-	-	-	-4.48	1.35	-1.94	-12.05	-2.33	-1.96	-	-	-	-	-	-	-
GLM-4.1V-9B-Thinking	Short	-0.78	-2.06	-2.35	0.05	0.40	-1.22	4.87	-1.10	-2.82	-0.89	-0.72	-1.46				
GLM-4.1V-9B-Thinking	Long	-	-	-	-0.51	1.08	0.79	-7.88	-5.70	-2.34	-	-	-	-	-	-	-
MiMo-VL-7B-RL	Short	14.69	-0.04	-0.95	-2.82	3.11	2.77	0.65	3.40	-4.95	0.38	0.36	-0.82				
MiMo-VL-7B-RL	Long	-	-	-	-2.29	3.51	3.07	6.39	3.92	0.01	-	-	-	-	-	-	-
Gemini-3.1-Pro	Short	2.54	3.72	-0.73	17.88	2.48	0.47	-1.81	2.05	0.05	0.05	0.60	-0.18				
Gemini-3.1-Pro	Long	-	-	-	-0.39	4.11	1.08	3.39	7.07	-0.43	-	-	-	-	-	-	-
GPT-5.4	Short	-1.79	-3.15	1.52	-14.97	1.86	-0.78	6.49	3.22	1.20	-0.29	-0.86	0.53				
GPT-5.4	Long	-	-	-	1.83	0.72	0.48	4.83	1.16	-2.01	-	-	-	-	-	-	-

Table 1: Coverage-based Directional Positional Bias (DPB) and Middle-Edge Gap (MEG) across domains and models. Negative DPB values indicate primacy, i.e., higher coverage for earlier positions, while positive values indicate recency, i.e., higher coverage for later positions. MEG is defined only for four-video inputs; negative MEG values indicate middle-position weakness.

**Middle-position weakness can be hidden by signed directional bias.** DPB alone does not capture non-monotonic position effects. Several settings with near-zero DPB still exhibit negative Middle-Edge Gap (MEG). For instance, InternVL3.5-14B on Leisure-4 (Short) has DPB 0.07% but MEG  $-2.65\%$ . Similarly, GLM-4.1V-9B-Thinking has DPB  $-1.10\%$  but MEG  $-2.82\%$ .

**Pairwise and listwise settings reveal different behavior.** Pairwise directional bias does not reliably predict four-video behavior. Several large  $P=2$  effects shrink or reverse under  $P=4$  inputs. For example, Qwen3-VL-8B changes from a strong recency pattern on Domestic-2 (Short,  $+8.13\%$ ) to nearly zero DPB on Domestic-4 (Short,  $-0.37\%$ ). InternVL3.5-8B moves from strong recency on Leisure-2 (Long,  $+13.89\%$ ) to mild primacy on Leisure-4 (Long,  $-1.28\%$ ). This suggests that listwise multi-video summarization introduces position interactions that are not visible in pairwise evaluation.

**Video duration changes the shape of positional effects.** This can occur because longer-duration settings use a larger sampled-frame budget, shifting the absolute input locations of later clips even when their relative slot indices are unchanged. In Domestic-4, several models show more negative MEG under longer inputs, such as Qwen3-VL-30B ( $-2.63\%$  to  $-3.68\%$ ) and InternVL3.5-14B ( $-2.11\%$  to  $-3.15\%$ ). In Leisure-4, negative MEG is common in both short and long settings, but some models change substantially: GPT-5.4 moves from positive MEG in the short setting ( $+1.20\%$ ) to neg-

ative MEG in the long setting ( $-2.01\%$ ). These patterns suggest that duration and visual context length can modulate positional effects, rather than simply amplifying a fixed primacy or recency bias.

**Case study.** Among the proprietary models, we observe strong directional positional effects in both Gemini-3.1-Pro and GPT-5.4 on Domestic-2 (Short). GPT-5.4 has DPB  $-14.97\%$  on Domestic-2 (Short), indicating substantially lower coverage for the second-position video. Manual inspection shows that the lower-scoring second-position summaries are often more generic, omitting concrete actions or object details. For example, summaries describing workers near a concrete or plaster machine were not judged as covering the reference phrase about men making plaster, and summaries mentioning a pit stop or loose tires were not judged as covering the specific action of changing tires.

This case also shows that small DPB values should be interpreted carefully. Near-zero DPB may reflect balanced coverage, but it may also occur when a model is uniformly generic and fails to cover all videos well. Stronger models may therefore exhibit larger measured positional bias because they preserve more details in favored positions, making uneven coverage easier to detect.

We also find that coverage differences can be accompanied by uneven output allocation. Table 2 shows Qwen3-VL-8B on Domestic-4 (Short). The middle slots have comparable word counts to the first slot but lower coverage, while the final slot is longer and more often exceeds the requested number of sentences.

Position	Avg. words	Over-rate	Coverage
Pos. 1	66.92	2.78%	0.4388
Pos. 2	66.60	1.85%	0.4118
Pos. 3	67.09	6.48%	0.4047
Pos. 4	69.68	8.33%	0.4290

Table 2: **Output allocation example for Qwen3-VL-8B on Domestic-4 (Short).** Over-rate denotes the proportion of outputs exceeding the requested number of sentences.

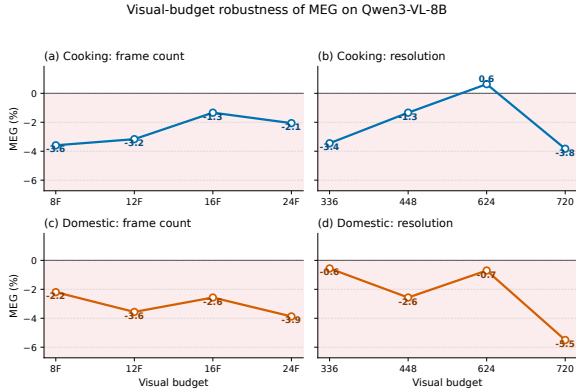


Figure 2: Visual-budget robustness check for Qwen3-VL-8B.

## 4.2 Visual-budget robustness.

We further examine whether the observed positional effect is an artifact of a particular visual input configuration. This analysis uses Qwen3-VL-8B on the  $P=4$  short-video setting. We vary the number of sampled frames while fixing the resolution at  $448 \times 448$ , and vary the resolution while fixing the frame count at 16. We report MEG (%), where negative values indicate that middle positions underperform edge positions.

Figure 2 shows that the negative MEG pattern is largely preserved under visual-budget changes. In *Domestic*, MEG remains negative under all tested settings.

We also run the same visual-budget ablation on MiMo-VL-7B-RL, whose more stable effect appears in Coverage: using only 8 frames reduces average Coverage across domains, while 24 frames improves it. We report the full MiMo ablation in Appendix C.3.

## 4.3 Requested Summary Budget and Middle-Position Weakness

We next test whether middle-position weakness is driven by the summary-length constraint in the prompt. A tight requested budget may force the model to omit details unevenly across positions.

Budget	Requested sent.	All outputs	Exact-budget
Short	2	-2.29	-0.63
Base	4	-2.45	-2.60
Long	6	-4.22	-3.70

Table 3: MEG for the Domestic-long setting under different requested summary budgets

We therefore vary the requested per-video budget with three settings: short, base, and long, corresponding to 1/2, 2/4, and 3/6 requested sentences for News/ActivityNet-based domains, respectively. For each four-video input, we compute MEG and also report an exact-budget subset whose generated sentence counts match the requested numbers.

Table 3 illustrates the pattern on Domestic-long. Under the short budget, the gap becomes much smaller in the exact-budget subset, suggesting that a tight two-sentence budget compresses all positions and can mask position-specific differences. With larger budgets, the gap remains negative even after sentence-count matching, and is largest in the long setting. Thus, giving the model more output space does not necessarily remove middle-position weakness; it can instead make uneven detail allocation more visible.

More broadly, increasing the requested budget does not benefit all positions equally. From short to long, middle positions receive smaller coverage gains than edge positions in four of six  $P = 4$  datasets. This suggests that the issue is not only whether the model writes enough sentences, but how added generation space is allocated across input positions.

## 4.4 Boundary-format Robustness

Prior multi-video benchmarks show that MLLMs can struggle to filter irrelevant information across videos in multi-video inputs (Peng et al., 2025). This makes input boundary design a relevant protocol factor: visual separators may help models segment videos, while text-only labels may change how strongly the model separates one video from another. We therefore compare the default black-frame separator with a text-label-only variant.

Overall, changing the boundary format affects the position-wise coverage curve, but does not provide a consistent improvement. For InternVL3.5-8B, the text-label-only format changes the curve more visibly: *Cooking* and *Domestic* show less negative MEG, but this does not translate into uniformly better summary quality. In *Domestic*, po-

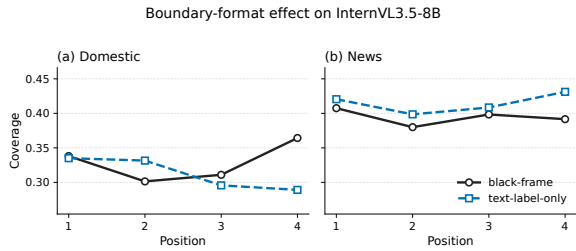


Figure 3: Boundary-format comparison for InternVL3.5-8B.

sition 2 improves while position 4 drops substantially, suggesting that text-only boundaries flatten the curve rather than consistently improving coverage. For Qwen3-VL-8B, removing black frames does not remove the middle-position weakness.

As a slot-boundary sanity check, we also compare each generated slot summary with its own reference and with the other references in the same group using TF-IDF content-token similarity. A slot is marked as potential contamination only when it is substantially more similar to another video’s reference than to its own. This proxy is not a verified leakage label, but it can reveal large-scale slot-boundary failures. We do not observe a systematic increase in potential contamination under text-label-only formatting.

## 5 Prompt-Level Mitigation and Diagnostics

We explore lightweight prompt-level interventions and diagnostics that do not require model retraining or architectural access. We first test an explicit balanced-attention instruction, then evaluate a single-target generation protocol, and finally examine prompt placement as a target-binding diagnostic.

### 5.1 Balanced-attention instruction.

We first add a direct instruction asking the model to allocate equal attention to each video. Figure 4 shows that this intervention does not provide reliable mitigation. For Qwen3-VL-8B, the equal-attention prompt does not produce a stable coverage balancing effect across positions. For InternVL3.5-8B, the Cooking curve becomes flatter, but this flattening partly comes from lowering edge-position coverage rather than uniformly improving all positions. Thus, the prompt can reshape the position-wise coverage curve, but does not consistently improve summary quality or remove posi-

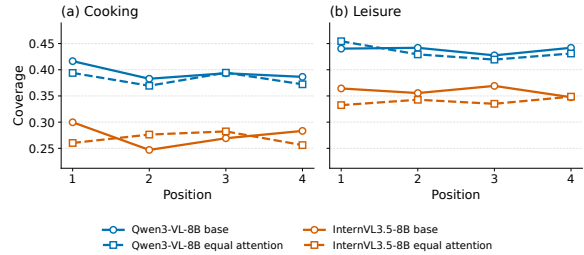


Figure 4: Effect of equal-attention prompting on position-wise coverage for Qwen3-VL-8B and InternVL3.5-8B.

tional imbalance.

### 5.2 Single-target Prompting

We also test a single-target generation protocol as an output-side diagnostic. The model receives the same multi-video input, but each call requests only one specified target-video summary instead of all summaries in one response. This removes previously generated summaries from the autoregressive prefix and tests whether position-dependent errors arise from joint generation effects, such as uneven detail allocation, or cross-summary contamination. If the bias persists, it is more likely due to the multi-video input itself; if it weakens, joint multi-summary generation may contribute to the effect.

**Target-addressing concern.** Single-target prompting introduces an additional target-addressing ambiguity that is less salient in joint per-video generation. Unlike joint generation, where the model outputs descriptions for all videos together, single-target prompting requires the model to resolve one specified label. We observe that models may confuse this label with ordinal position: even when the prompt explicitly states which frames correspond to each label, video[1] can still be treated as the first or currently queried video rather than the second zero-indexed video.

To quantify this label-resolution issue, we compute TF-IDF cosine similarity between each generated summary and the four references in the same group. A target hit occurs when the true target reference has the highest similarity; a margin confusion occurs when another reference exceeds the true target by over 0.05. Table 4 shows that one-indexed labels mainly improve target addressing at position 2, where zero-indexing is most ambiguous. We therefore compare zero-indexed and one-indexed labels on InternVL3.5-14B to test whether this addressing convention contributes to the single-target effect.

Target pos.	$\Delta$ Coverage	$\Delta$ Target hit	$\Delta$ Margin confusion
Pos. 1	-0.54	-0.23	-0.93
Pos. 2	+4.18	+14.12	-11.81

Table 4: Effect of changing single-target labels from zero-indexed to one-indexed form on InternVL3.5-14B.

Scale	$\Delta$ Weak Cov.	$\Delta$ Weak Sent.	Weak pos. imp.	$\Delta$ Density
$P=2$	-4.09	+0.16	0/6	-0.121
$P=4$	+2.87	+1.26	4/6	-0.224

Table 5: Effect of single-target prompting relative to joint generation for InternVL3.5-14B. Weak positions are identified from the joint-generation setting.  $\Delta$ Density is the change in coverage per 100 words.

**Effect analysis.** Table 5 shows a scale-dependent effect. For  $P=4$ , single-target prompting improves the weak-position coverage by 2.87 percentage points and improves the weakest joint-generation position in 4 of 6 datasets. The gain is accompanied by a much larger sentence increase, especially for positions that were compressed in the joint output.

In contrast, for  $P=2$ , the weak-position coverage decreases despite a small increase in generated sentences. Overall, this protocol is not a general summarization improvement, but a possible inference-time workaround when the number of input videos grows and joint generation begins to compress some summary slots.

### 5.3 Prompt Placement and Leakage Audit

We next examine whether prompt placement affects target binding. In the main setting, the task instruction appears before the videos, while a video-first variant places the same instruction after the videos. We first inspect the easier  $P=2$  setting, where inputs are shorter and model performance is generally stronger. For InternVL3.5-14B, video-first produces slightly longer ActivityNet outputs on average (3.817 vs. 3.667 sentences), but reduces  $P=2$  coverage by 4.29 points. This suggests that prompt placement affects target binding, not merely instruction compliance.

To further test this target-binding concern, we conduct a targeted leakage audit. A full target-alignment audit would require comparing thousands of generated summaries with their corresponding videos. Instead, we use a reference-based candidate miner to reduce the review space. The miner is designed around the observation that cross-video leakage often appears as a concrete action or object detail from another video, even when

Protocol	Cand. sent.	Verified leak	Cand. prec.	Slot rate	Sent. rate
Prompt-first	263	52	19.77%	1.93%	0.68%
Video-first	446	96	21.52%	3.56%	0.93%

Table 6: Manual verification of candidate cross-video leakage under prompt-placement variants. Cand. sent. denotes mined candidate sentences; Verified leak denotes manually confirmed leakage sentences; Cand. prec. is Verified leak / Cand. sent.

clips have similar scenes. For each generated sentence, it compares concrete action/object anchor words against the reference of the claimed target video and the references of the other videos in the same group. A sentence is selected as a candidate when its concrete evidence is weakly supported by the claimed target but better supported by another video. We then manually inspect these candidates against the videos and count a verified leak only when the sentence describes another input video.

Table 6 shows that video-first prompting produces more mined candidates and more manually verified leakage sentences than prompt-first prompting. At the position level, candidate precision is higher for positions 2 and 3 than for positions 1 and 4 under both prompt placements. We observe two recurring failure modes: full target-addressing failures, where the summary is assigned to the wrong video, and local detail intrusions, where the summary mostly describes the target video but borrows a concrete action or object from another video. Since one target-addressing error can affect multiple generated sentences, sentence-level counts may overstate the number of independent leakage events.

## 6 Conclusion

We present a systematic study of positional bias in multi-video summarization for MLLMs. Our results show that current models are not reliably position-invariant: summary quality varies with input order across domains, model families, and input settings. We further show that signed directional bias alone is insufficient, since low DPB can still hide middle-position weakness under MEG. Robustness and protocol analyses suggest that these effects are not reducible to a single artifact, while lightweight prompt-level interventions only partially reshape them. Our benchmark, metrics, and diagnostics provide a foundation for studying and improving order robustness in multi-video summarization.

## 7 Limitations

**Input scale and domains.** Our main experiments focus on inputs of up to four videos and clips within the 0–2 minute range from selected scenario categories. Positional effects under longer video lists, longer clips, or more open-ended video mixtures remain open questions.

**Evaluation scope.** Our coverage scores depend on human-written references. ActivityNet-derived domains and News also use different coverage estimators because their reference granularities differ, so absolute scores should be compared within each dataset family rather than across families. Our leakage audits are diagnostic and candidate-based, not exhaustive annotations of all generated content.

**Mechanistic and intervention scope.** We mainly provide behavioral and protocol-level analyses. Although our ablation and mitigation experiments identify factors that reshape positional effects, they do not provide a full causal mechanism. Also, stronger mitigation may require training-time or architectural interventions beyond lightweight prompting.

## 8 Potential Risks

A potential risk of this work is that positional bias may be misused to place preferred videos in fixed positions, thereby shaping summary emphasis and causing overexposure of some content while reducing the visibility of others.

## References

- Purui Bai, Tao Wu, Jiayang Sun, Xinyue Liu, Huaibo Huang, and Ran He. 2026. [Mvpbench: A multi-video perception evaluation benchmark for multi-modal video understanding](#). *Preprint*, arXiv:2603.22756.
- Shuai Bai, Yuxuan Cai, Ruizhe Chen, Keqin Chen, Xionghui Chen, Zesen Cheng, Lianghao Deng, Wei Ding, Chang Gao, Chunjiang Ge, Wenbin Ge, Zhifang Guo, Qidong Huang, Jie Huang, Fei Huang, Binyuan Hui, Shutong Jiang, Zhaohai Li, Mingsheng Li, and 45 others. 2025. [Qwen3-vl technical report](#). *Preprint*, arXiv:2511.21631.
- Satanjeev Banerjee and Alon Lavie. 2005. [METEOR: An automatic metric for MT evaluation with improved correlation with human judgments](#). In *Proceedings of the ACL Workshop on Intrinsic and Extrinsic Evaluation Measures for Machine Translation and/or Summarization*, pages 65–72, Ann Arbor, Michigan. Association for Computational Linguistics.
- Yupeng Chang, Xu Wang, Jindong Wang, Yuan Wu, Linyi Yang, Kaijie Zhu, Hao Chen, Xiaoyuan Yi, Cunxiang Wang, Yidong Wang, Wei Ye, Yue Zhang, Yi Chang, Philip S. Yu, Qiang Yang, and Xing Xie. 2024. [A survey on evaluation of large language models](#). *ACM Trans. Intell. Syst. Technol.*, 15(3).
- Paul Covington, Jay Adams, and Emre Sargin. 2016. [Deep neural networks for youtube recommendations](#). In *Proceedings of the 10th ACM Conference on Recommender Systems, RecSys '16*, pages 191–198, New York, NY, USA. Association for Computing Machinery.
- Junbo Cui, Bokai Xu, Chongyi Wang, Tianyu Yu, Weiyue Sun, Yingjing Xu, Tianran Wang, Zhihui He, Wenshuo Ma, Tianchi Cai, Jiancheng Gui, Luoyuan Zhang, Xian Sun, Fuwei Huang, Moye Chen, Zhuo Lin, Hanyu Liu, Qingxin Gui, Qingzhe Han, and 17 others. 2026. [Minicpm-o 4.5: Towards real-time full-duplex omni-modal interaction](#). *Preprint*, arXiv:2604.27393.
- Jinlan Fu, See-Kiong Ng, Zhengbao Jiang, and Pengfei Liu. 2024. [GPTScore: Evaluate as you desire](#). In *Proceedings of the 2024 Conference of the North American Chapter of the Association for Computational Linguistics: Human Language Technologies (Volume 1: Long Papers)*, pages 6556–6576, Mexico City, Mexico. Association for Computational Linguistics.
- Google DeepMind. 2026. [Gemini 3.1 pro model card](#).
- Matt Grenander, Yue Dong, Jackie Chi Kit Cheung, and Annie Louis. 2019. [Countering the effects of lead bias in news summarization via multi-stage training and auxiliary losses](#). In *Proceedings of the 2019 Conference on Empirical Methods in Natural Language Processing and the 9th International Joint Conference on Natural Language Processing (EMNLP-IJCNLP)*, pages 6019–6024, Hong Kong, China. Association for Computational Linguistics.
- Max Grusky, Mor Naaman, and Yoav Artzi. 2018. [Newsroom: A dataset of 1.3 million summaries with diverse extractive strategies](#). In *Proceedings of the 2018 Conference of the North American Chapter of the Association for Computational Linguistics: Human Language Technologies, Volume 1 (Long Papers)*, pages 708–719, New Orleans, Louisiana. Association for Computational Linguistics.
- Fabian Caba Heilbron, Victor Escorcia, Bernard Ghanem, and Juan Carlos Nibbles. 2015. [ActivityNet: A large-scale video benchmark for human activity understanding](#). In *2015 IEEE Conference on Computer Vision and Pattern Recognition (CVPR)*, pages 961–970.
- Yupeng Hou, Junjie Zhang, Zihan Lin, Hongyu Lu, Ruobing Xie, Julian McAuley, and Wayne Xin Zhao. 2024. [Large language models are zero-shot rankers for recommender systems](#). *Preprint*, arXiv:2305.08845.

- Woojun Jung and Junyeong Kim. 2025. **QEVA: A reference-free evaluation metric for narrative video summarization with multimodal question answering**. In *Findings of the Association for Computational Linguistics: EMNLP 2025*, pages 24632–24642, Suzhou, China. Association for Computational Linguistics.
- Kajal Kansal, Nikita Kansal, Sreevaatsav Bavana, Bodla Krishna Vamshi, and Nidhi Goyal. 2023. **A systematic study on video summarization: Approaches, challenges, and future directions**. In *Proceedings of the 2nd Workshop on User-Centric Narrative Summarization of Long Videos, NarSUM '23*, page 65–73, New York, NY, USA. Association for Computing Machinery.
- Ryan Koo, Minhwa Lee, Vipul Raheja, Jong Inn Park, Zae Myung Kim, and Dongyeop Kang. 2024. **Benchmarking cognitive biases in large language models as evaluators**. In *Findings of the Association for Computational Linguistics: ACL 2024*, pages 517–545, Bangkok, Thailand. Association for Computational Linguistics.
- Chin-Yew Lin. 2004. **ROUGE: A package for automatic evaluation of summaries**. In *Text Summarization Branches Out*, pages 74–81, Barcelona, Spain. Association for Computational Linguistics.
- Nelson F. Liu, Kevin Lin, John Hewitt, Ashwin Paranjape, Michele Bevilacqua, Fabio Petroni, and Percy Liang. 2024. **Lost in the middle: How language models use long contexts**. *Transactions of the Association for Computational Linguistics*, 12:157–173.
- Yang Liu, Dan Iter, Yichong Xu, Shuhang Wang, Ruo Chen Xu, and Chenguang Zhu. 2023. **G-eval: NLG evaluation using gpt-4 with better human alignment**. In *Proceedings of the 2023 Conference on Empirical Methods in Natural Language Processing*, pages 2511–2522, Singapore. Association for Computational Linguistics.
- OpenAI. 2025. Gpt-5.1 instant and gpt-5.1 thinking system card addendum. [https://cdn.openai.com/pdf/4173ec8d-1229-47db-96de-06d87147e07e/5\\_1\\_system\\_card.pdf](https://cdn.openai.com/pdf/4173ec8d-1229-47db-96de-06d87147e07e/5_1_system_card.pdf).
- OpenAI. 2026. GPT-5.4 Thinking System Card. <https://openai.com/index/gpt-5-4-thinking-system-card/>.
- Kishore Papineni, Salim Roukos, Todd Ward, and Wei-Jing Zhu. 2002. **Bleu: a method for automatic evaluation of machine translation**. In *Proceedings of the 40th Annual Meeting of the Association for Computational Linguistics*, pages 311–318, Philadelphia, Pennsylvania, USA. Association for Computational Linguistics.
- Tianhao Peng, Haochen Wang, Yuanxing Zhang, Zekun Moore Wang, Zili Wang, Ge Zhang, Jian Yang, Shihao Li, Yanghai Wang, Xintao Wang, Houyi Li, Wei Ji, Pengfei Wan, Wenhao Huang, Zhaoxiang Zhang, and Jiaheng Liu. 2025. **MVU-eval: Towards multi-video understanding evaluation for multimodal LLMs**. In *The Thirty-ninth Annual Conference on Neural Information Processing Systems Datasets and Benchmarks Track*.
- Clement Rebuffel, Thomas Scialom, Laure Soulier, Benjamin Piwowarski, Sylvain Lamprier, Jacopo Staiano, Geoffrey Scuttheeten, and Patrick Gallinari. 2021. **Data-QuestEval: A referenceless metric for data-to-text semantic evaluation**. In *Proceedings of the 2021 Conference on Empirical Methods in Natural Language Processing*, pages 8029–8036, Online and Punta Cana, Dominican Republic. Association for Computational Linguistics.
- Patrick Schilcher, Dominik Karasin, Michael Schöpf, Haisam Saleh, Antonela Tommasel, and Markus Schedl. 2025. **Characterizing positional bias in large language models: A multi-model evaluation of prompt order effects**. In *Findings of the Association for Computational Linguistics: EMNLP 2025*, pages 20643–20664, Suzhou, China. Association for Computational Linguistics.
- Lin Shi, Chiyu Ma, Wenhua Liang, Xingjian Diao, Weicheng Ma, and Soroush Vosoughi. 2025. **Judging the judges: A systematic study of position bias in LLM-as-a-judge**. In *Proceedings of the 14th International Joint Conference on Natural Language Processing and the 4th Conference of the Asia-Pacific Chapter of the Association for Computational Linguistics*, pages 292–314, Mumbai, India. The Asian Federation of Natural Language Processing and The Association for Computational Linguistics.
- Aaron Smith, Skye Toor, and Patrick van Kessel. 2018. **Many turn to youtube for children’s content, news, how-to lessons**. Technical report, Pew Research Center.
- V Team, Wenyi Hong, Wenmeng Yu, Xiaotao Gu, Guo Wang, Guobing Gan, Haomiao Tang, Jiale Cheng, Ji Qi, Junhui Ji, Lihang Pan, Shuaiqi Duan, Weihang Wang, Yan Wang, Yean Cheng, Zehai He, Zhe Su, Zhen Yang, Ziyang Pan, and 74 others. 2026. **Glm-4.5v and glm-4.1v-thinking: Towards versatile multimodal reasoning with scalable reinforcement learning**. Preprint, arXiv:2507.01006.
- Xinyu Tian, Shu Zou, Zhaoyuan Yang, and Jing Zhang. 2025. **Identifying and mitigating position bias of multi-image vision-language models**. In *Proceedings of the Computer Vision and Pattern Recognition Conference*, pages 10599–10609.
- David Wan, Jesse Vig, Mohit Bansal, and Shafiq Joty. 2025. **On positional bias of faithfulness for long-form summarization**. In *Proceedings of the 2025 Conference of the Nations of the Americas Chapter of the Association for Computational Linguistics: Human Language Technologies (Volume 1: Long Papers)*, pages 8791–8810, Albuquerque, New Mexico. Association for Computational Linguistics.
- Peiyi Wang, Lei Li, Liang Chen, Zefan Cai, Dawei Zhu, Binghui Lin, Yunbo Cao, Lingpeng Kong,

- Qi Liu, Tianyu Liu, and Zhifang Sui. 2024. [Large language models are not fair evaluators](#). In *Proceedings of the 62nd Annual Meeting of the Association for Computational Linguistics (Volume 1: Long Papers)*, pages 9440–9450, Bangkok, Thailand. Association for Computational Linguistics.
- Weiyun Wang, Zhangwei Gao, Lixin Gu, Hengjun Pu, Long Cui, Xingguang Wei, Zhaoyang Liu, Linglin Jing, Shenglong Ye, Jie Shao, Zhaokai Wang, Zhe Chen, Hongjie Zhang, Ganlin Yang, Haomin Wang, Qi Wei, Jinhui Yin, Wenhao Li, Erfei Cui, and 56 others. 2025. [InternV3.5: Advancing open-source multimodal models in versatility, reasoning, and efficiency](#). *Preprint*, arXiv:2508.18265.
- Spencer Whitehead, Heng Ji, Mohit Bansal, Shih-Fu Chang, and Clare Voss. 2018. [Incorporating background knowledge into video description generation](#). In *Proceedings of the 2018 Conference on Empirical Methods in Natural Language Processing*, pages 3992–4001, Brussels, Belgium. Association for Computational Linguistics.
- Hou Xia, Zheren Fu, Fangcan Ling, Jiajun Li, Yi Tu, Zhendong Mao, and Yongdong Zhang. 2025. [Video-level gauge: Investigating contextual positional bias in large video language models](#). *Preprint*, arXiv:2508.19650.
- LLM-Core-Team Xiaomi. 2025. [Mimo-vl technical report](#). *Preprint*, arXiv:2506.03569.
- Tianyi Zhang, Varsha Kishore, Felix Wu, Kilian Q. Weinberger, and Yoav Artzi. 2020. [Bertscore: Evaluating text generation with bert](#). *Preprint*, arXiv:1904.09675.
- Zhenyu Zhang, Runjin Chen, Shiwei Liu, Zhewei Yao, Olatunji Ruwase, Beidi Chen, Xiaoxia Wu, and Zhangyang Wang. 2024. [Found in the middle: How language models use long contexts better via plug-and-play positional encoding](#). In *Advances in Neural Information Processing Systems*, volume 37, pages 60755–60775. Curran Associates, Inc.
- Junjie Zhou, Yan Shu, Bo Zhao, Boya Wu, Zhengyang Liang, Shitao Xiao, Minghao Qin, Xi Yang, Yongping Xiong, Bo Zhang, Tiejun Huang, and Zheng Liu. 2025. [Mlvu: Benchmarking multi-task long video understanding](#). In *2025 IEEE/CVF Conference on Computer Vision and Pattern Recognition (CVPR)*, pages 13691–13701.

## A Prompts and LLM as a judge

### A.1 Per-video Summarization Prompts

We use a fixed per-video output structure to support reliable slot extraction and position-wise analysis. In the main experiments, the task prompt is placed before the visual inputs. For ActivityNet-based domains, we request four sentences per video. For the News domain, whose references are much shorter, we request two sentences per news video. The required output markers are zero-indexed and extend to the number of videos in the input, e.g., [video0] through [video3] for four-video inputs.

#### Main black-frame prompt.

Different videos in the input are separated by black frames.  
Summarize each video in 4 sentences.  
Use exactly this format, including the square brackets:  
[video0] summary  
[video1] summary  
...  
[video{P-1}] summary  
*Input layout:*  
Video 0: {N} uniformly sampled frames  
{frames of video 0}  
<black separator>  
Video 1: {N} uniformly sampled frames  
{frames of video 1}  
<black separator>  
...  
Video {P-1}: {N} uniformly sampled frames  
{frames of video {P-1}}

#### Text-label-only prompt.

Different videos in the input are separated by text labels only.  
Summarize each video in 4 sentences.  
Use exactly this format, including the square brackets:  
[video0] summary  
[video1] summary  
...  
[video{P-1}] summary  
*Input layout:*  
Video 0: {N} uniformly sampled frames  
{frames of video 0}  
- Text separator: end of Video 0; next is Video 1. -  
Video 1: {N} uniformly sampled frames  
{frames of video 1}  
- Text separator: end of Video 1; next is Video 2. -  
...  
Video {P-1}: {N} uniformly sampled frames  
{frames of video {P-1}}

For News, the second line is again replaced by Summarize each news video in 2 sentences.

### A.2 LLM-as-a-Judge Prompt for Sentence-level Coverage

We evaluate ActivityNet Coverage using an LLM-as-a-Judge protocol with gpt-5.1-2025-11-13. Given a reference summary split into sentences and a model-generated summary for the same video, the judge returns a binary covered/not-covered decision for each reference sentence. We use the following prompt with temperature 0.

You are evaluating whether a model-generated video summary covers a human reference summary. For EACH reference sentence, decide whether it is clearly covered by the model-generated summary.

Scoring rule:

- covered = 1 if the model summary explicitly or implicitly describes the same fact as the reference sentence.
- covered = 0 if the model summary omits the key information, contradicts the reference sentence, or is too vague/general to support the specific reference sentence.

Rules:

- Different wording is acceptable when the meaning matches.
- Do not require exact phrasing.
- If only part of a reference sentence is covered and an important fact is missing, score 0.
- For covered=0, explain briefly what is missing or contradicted.
- For covered=1, reason must be an empty string.

Reference sentences:

{numbered\_refs}

Model-generated summary:

{model\_summary}

Return ONLY valid JSON. Do not include markdown.

Required JSON schema:

```
{
  "sentence_scores": [
    {"index": 1, "covered": 1, "reason": ""},
    {"index": 2, "covered": 0, "reason": "The model summary does not mention ..."}
  ]
}
```

### A.3 Human Agreement and Judge Robustness

To assess the reliability of the sentence-level coverage judge, we recruited three undergraduate annotators and compensated them at a rate of USD 8 per hour to conduct a human agreement check on 240 annotated items. Each annotator independently scored coverage, and we compare pairwise human agreement with the agreement between the LLM judge and the mean human score. Table 7 reports

Comparison	$n$	Pearson	Spearman
Annotator 1 vs. Annotator 2	240	0.7760	0.7651
Annotator 1 vs. Annotator 3	240	0.7152	0.7138
Annotator 2 vs. Annotator 3	240	0.7765	0.7796
Human mean vs. LLM	240	0.7116	0.6985

Table 7: Human agreement and LLM-judge robustness for sentence-level coverage scoring. The LLM judge shows a positive correlation with the mean human score.

Pearson and Spearman correlations.

The LLM judge is not a perfect substitute for human annotation, but its agreement with the mean human score is comparable to the lower end of human-human agreement. We therefore use it as a scalable coverage estimator for large-scale positional analysis, while treating individual borderline cases with caution.

## B Dataset Licenses and Usage Conditions

Our benchmark is constructed from two publicly available third-party datasets derived from web videos: the News Video Dataset and ActivityNet. For the News Video Dataset, the official repository states that the dataset is released for educational and research purposes only, while the videos remain protected under their respective YouTube licenses and belong to their original copyright holders. For ActivityNet, we rely on the official release of the dataset and the access channels provided by the benchmark creators.

## C More Experimental Details

**Computational budget.** All local experiments were conducted on NVIDIA RTX PRO 6000 GPUs with 96GB memory. Qwen3-VL-30B-A3B and InternVL3.5-14B were run with three GPUs, while the other locally evaluated models were run with a single GPU. Across local inference and automatic evaluation runs, the total computational budget was approximately 1,100 GPU-hours.

### C.1 Parsing and Output-Failure Diagnostics

We also inspect whether positional effects are confounded by parsing or complete output failures. Most models follow the requested [videoX] format. We distinguish two failure modes. A *marker failure* occurs when the model attempts the fixed marker format but misses or malforms one or more required video slots; such cases are marked as failures for the affected slots. A *fallback* case occurs only when the model does not follow the

Model	Marker fail.	Fallback
Qwen3-VL-8B	1	1
InternVL3.5-8B	5	1
InternVL3.5-14B	8	0
Qwen3-VL-30B-A3B	1	0
MiMo-VL-7B-RL	14	3

Table 8: Marker parsing failures in the baseline records.

Setting	Failures
Cooking-2	3
Cooking-4	22
Domestic-S-2	6
Domestic-S-4	24
Domestic-L-2	7
Domestic-L-4	22
Leisure-S-2	10
Leisure-S-4	28
Leisure-L-2	8
Leisure-L-4	36

Table 9: MiMo-VL-7B-RL complete output failures.

fixed marker format at all, in which case we use BERTScore sentence assignment to recover a best-effort alignment. Table 8 reports only failure counts.

Complete output failures are more concentrated. Table 9 shows the MiMo-VL-7B-RL settings where the model produced placeholder-only outputs, such as literal [video0] summary-style text, rather than substantive descriptions of the videos. These outputs are unusable for coverage evaluation and are assigned zero Coverage in the baseline aggregation. These failures occur mainly in ActivityNet settings and become more frequent in four-video inputs.

### C.2 Coverage Curves for All Baseline Models

Figures 5 and 6 report the full baseline Coverage–position curves. We split models into two groups only for readability; both figures use the same ordering of domains, durations, and input scales.

Some Gemini-3.1-Pro settings have lower Coverage despite fluent summaries. This reflects the intended scope of our metric rather than a global judgment of summary quality. Coverage is reference-grounded: since summaries are ultimately intended for human readers, we assume that human-written references identify the salient facts and events that readers expect a summary to preserve. Our inspection suggests that Gemini-3.1-Pro often produces shorter and more abstractive summaries, which may contain fewer explicit reference-grounded details under this metric. This limitation does not undermine the positional analysis, because we com-

pare Coverage across input slots under the same scoring rule. If reference-grounded information preservation varies by slot, the model still exhibits order-dependent summarization behavior.

### C.3 Visual-budget Ablation Tables

The main text reports a visual-budget robustness check for Qwen3-VL-8B. Here we provide the full visual-budget summaries for Qwen3-VL-8B and MiniCPM-o-4.5, including Coverage, DPB, and MEG. For Qwen3-VL-8B, negative MEG is largely preserved across frame-count and resolution variants, especially in *Domestic*. MiniCPM-o-4.5 shows a different pattern: frame count mainly changes overall Coverage, with 8 frames lowering Coverage and 24 frames improving Coverage across domains, while MEG remains mixed. These results support the main-text conclusion that larger visual budgets do not necessarily remove positional imbalance.

### C.4 InternVL3.5-14B Single-target All-dataset Results

Tables 11 and 12 provide the dataset-level results behind the single-target analysis in Section 5.2. The tables separate mean Coverage changes from weak-position changes. Single-target prompting lowers mean Coverage in all six  $P=2$  settings, but improves mean Coverage in all six  $P=4$  settings. The weak-position analysis shows the same scale dependence: none of the  $P=2$  weak positions improves, while 4 of 6  $P=4$  weak positions improve.

### C.5 Equal-attention Coverage Curves

Figure 7 reports the equal-attention prompt intervention on all four short four-video domains for Qwen3-VL-8B and InternVL3.5-8B. These curves complement the main-text two-domain visualization and show that the prompt intervention is model- and domain-dependent rather than a uniform fix for positional imbalance.

### C.6 Cyclic Versus Full-Permutation Ordering

The main experiments use cyclic orderings rather than full permutations. This design ensures that each video appears at each absolute position exactly once, while keeping inference and evaluation cost manageable. This trade-off is important: the current study already required roughly 1,100 hours for model inference and evaluation, and a full-permutation design would multiply the four-video setting from 4 cyclic orders to  $4! = 24$  orders

before considering models, domains, robustness settings, and judge-based scoring. The limitation is that cyclic ordering cannot fully average over surrounding context: absolute position effects may still be partially entangled with which videos appear before or after the target video.

Dataset	Cyclic MEG	Full MEG	Mean $ \Delta_{\text{pos}} $
Cooking	-1.34	-1.39	1.18
Domestic	-2.57	-0.49	1.04
Leisure	-0.64	+0.20	1.10
News	+0.15	+0.03	0.71

Table 13: **Cyclic versus full-permutation comparison for Qwen3-VL-8B.** MEG and mean absolute position-wise Coverage differences are reported in percentage points.

To assess this trade-off, Figure 8 compares Qwen3-VL-8B under the cyclic design and a full-permutation design on the short four-video setting. Full permutation separates three sources that are partially entangled in cyclic runs: absolute target position, surrounding video-order context, and residual generation or evaluation noise. The full-permutation results make the cyclic middle-position weakness slightly weaker on average: mean MEG changes from  $-1.10$  percentage points under cyclic ordering to  $-0.41$  percentage points under full permutation. However, the cyclic estimate remains a useful approximation for the main positional trend. The average absolute difference between cyclic and full-permutation position means is small, ranging from 0.71 to 1.18 percentage points across domains. The strongest cyclic middle weakness appears in *Domestic*, where full permutation reduces the magnitude but does not turn it into a strong middle advantage. *Cooking* remains negative under both designs, while *Leisure* and *News* are near zero under both. Overall, the check suggests that cyclic ordering can slightly overstate middle weakness in some domains, but does not produce a qualitatively different position curve in the current Qwen3-VL-8B setting.

## D Examples

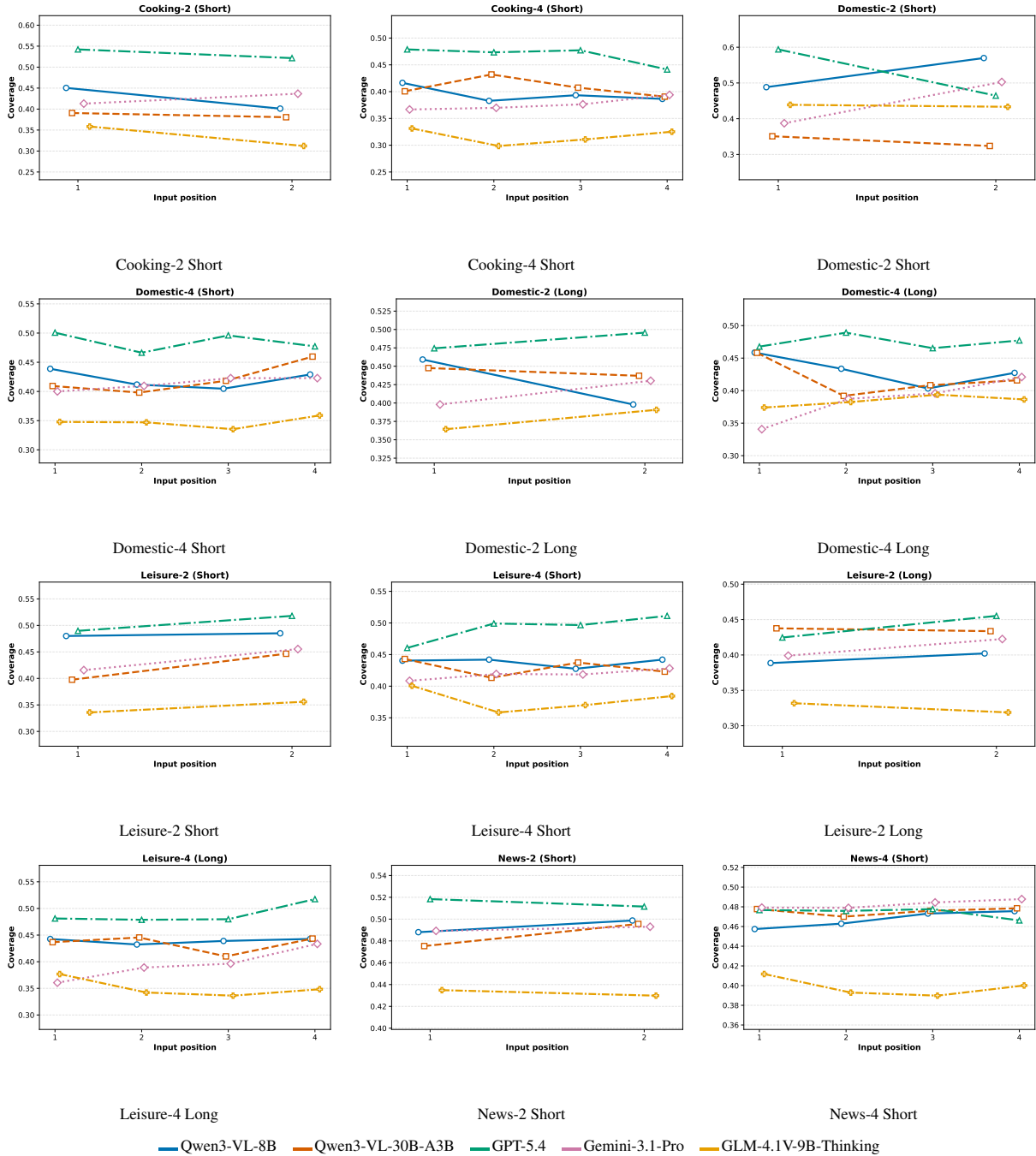


Figure 5: Baseline Coverage–position curves for model group A. Each panel corresponds to one domain, duration, and input-size setting.

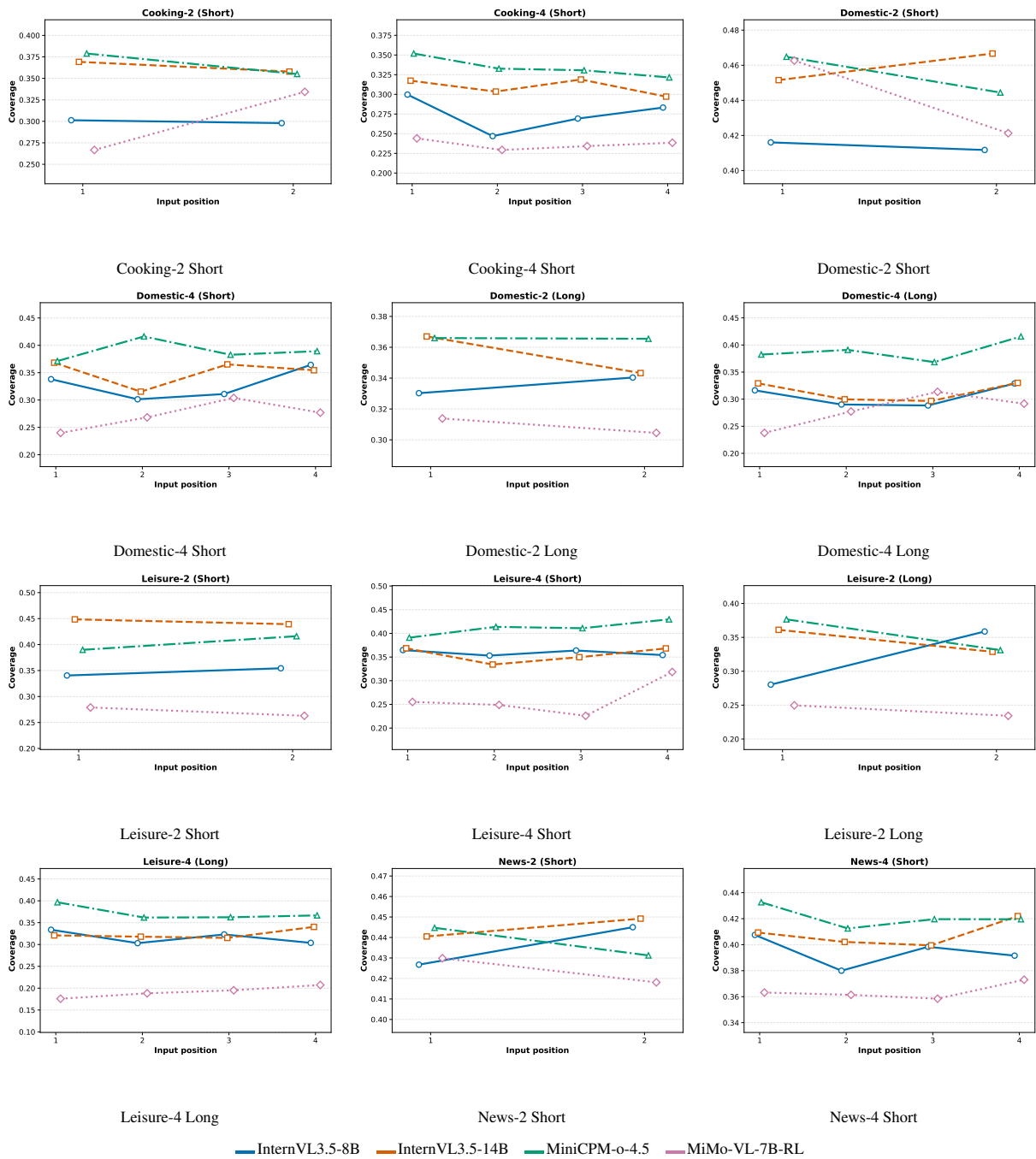


Figure 6: Baseline Coverage–position curves for model group B. The panel order matches Figure 5.

(a) Qwen3-VL-8B									(b) MiniCPM-o-4.5								
Domain	Metric	Base	8F	12F	24F	336R	624R	720R	Domain	Metric	Base	8F	12F	24F	336R	624R	720R
Cooking	Cov.	39.48	32.07	36.73	38.18	35.62	41.03	38.90	Cooking	Cov.	34.23	30.01	34.48	38.04	32.70	34.93	35.49
	DPB	-1.68	2.55	-0.19	-0.27	0.51	1.38	1.80		DPB	-0.58	0.49	1.00	-0.39	-0.30	0.39	-0.42
	MEG	-1.34	-3.59	-3.17	-2.06	-3.45	0.63	-3.83		MEG	-2.03	-2.42	-1.79	0.40	-0.65	-3.06	1.02
Domestic	Cov.	42.11	37.32	40.47	42.59	39.01	41.09	42.64	Domestic	Cov.	39.35	34.38	34.96	40.85	41.93	41.84	40.83
	DPB	-0.72	-2.70	0.69	0.07	-1.17	3.57	-0.81		DPB	0.79	0.90	-2.27	0.47	-0.35	-3.42	1.61
	MEG	-2.57	-2.20	-3.56	-3.87	-0.56	-0.70	-5.50		MEG	0.86	-1.45	0.52	-1.35	-0.58	-1.48	3.31
Leisure	Cov.	43.79	38.08	39.81	43.68	42.33	44.23	43.71	Leisure	Cov.	40.90	35.00	39.54	42.70	40.42	40.89	40.29
	DPB	-0.18	2.22	-2.23	0.37	0.48	0.83	0.53		DPB	-0.32	-2.13	-1.84	-1.10	0.64	-0.43	-0.00
	MEG	-0.64	-1.13	-1.49	-0.19	-3.12	-1.89	-0.10		MEG	-0.85	0.81	-0.96	-1.05	-1.34	-2.36	0.01
News	Cov.	46.73	37.14	44.78	47.04	45.92	46.27	45.87	News	Cov.	42.05	31.20	39.01	42.51	41.54	41.43	42.05
	DPB	1.16	0.07	0.95	0.85	0.51	0.21	0.37		DPB	-0.45	-2.45	-1.17	0.19	-0.60	-0.00	-0.58
	MEG	0.15	1.27	0.49	-0.24	0.34	-1.00	1.30		MEG	-1.19	-0.78	0.60	-1.18	-0.16	-1.04	-0.10

Table 10: Visual-budget ablation summary for Qwen3-VL-8B and MiniCPM-o-4.5 on short  $P=4$  settings. All values are percentages. Base denotes 16 frames at  $448 \times 448$ . Frame-count variants fix resolution at  $448 \times 448$ ; resolution variants fix frame count at 16.

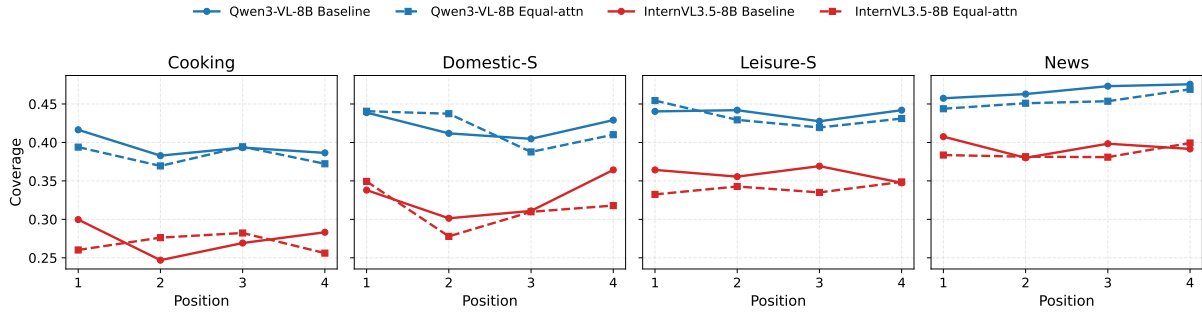


Figure 7: **Equal-attention prompt Coverage curves across all short four-video domains.** Solid lines are baseline prompt-first black-frame runs; dashed lines add the explicit equal-attention instruction.

Domain	Dur.	$P$	Joint	Single	Gain
Cooking	S	2	0.3635	0.3113	-5.22
Cooking	S	4	0.3092	0.3181	+0.88
Domestic	L	2	0.3551	0.3193	-3.59
Domestic	L	4	0.3139	0.3148	+0.09
Domestic	S	2	0.4591	0.4289	-3.02
Domestic	S	4	0.3508	0.3617	+1.09
News	S	2	0.4449	0.4384	-0.65
News	S	4	0.4082	0.4350	+2.68
Leisure	L	2	0.3449	0.3074	-3.75
Leisure	L	4	0.3235	0.3287	+0.52
Leisure	S	2	0.4439	0.3875	-5.63
Leisure	S	4	0.3552	0.4006	+4.54

Table 11: Dataset-level mean Coverage for InternVL3.5-14B under joint generation and single-target prompting. Gain is single-target minus joint generation, reported in percentage points.

Domain	Dur.	Weak pos.	Weak gain	Nonweak gain	Diff.
Cooking	S	pos4	+5.29	-0.59	+5.88
Domestic	L	pos3	-0.07	+0.15	-0.22
Domestic	S	pos2	+3.66	+0.23	+3.43
News	S	pos3	+4.15	+2.18	+1.97
Leisure	L	pos3	-0.90	+0.99	-1.89
Leisure	S	pos2	+5.07	+4.36	+0.71

Table 12: Weak-position gain for InternVL3.5-14B in  $P=4$  settings. The weak position is the lowest-Coverage position under joint generation. Gains are single-target minus joint generation, reported in percentage points. Diff. is weak-position gain minus the average gain of the remaining positions.

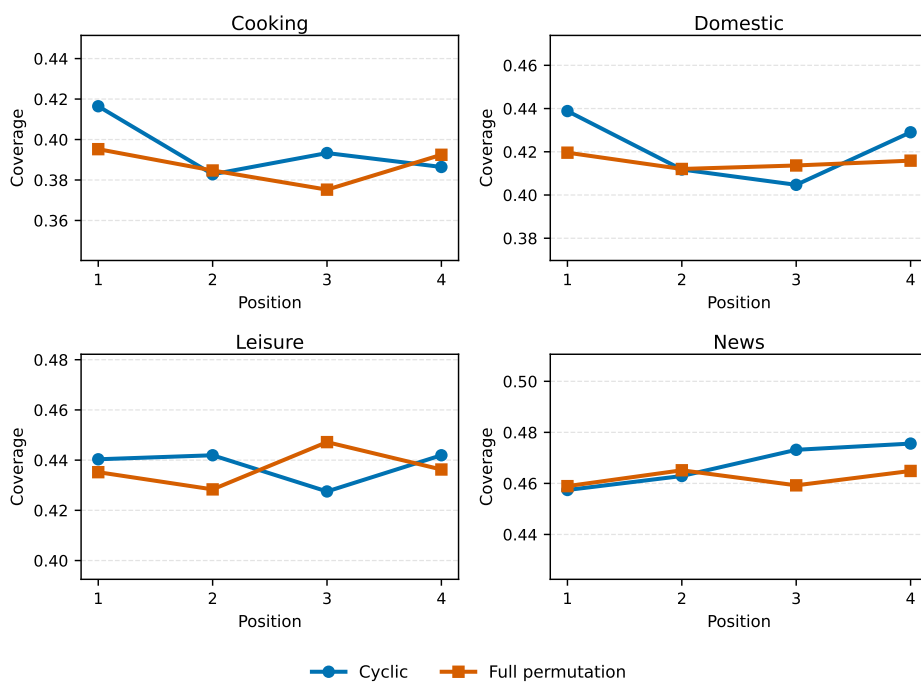
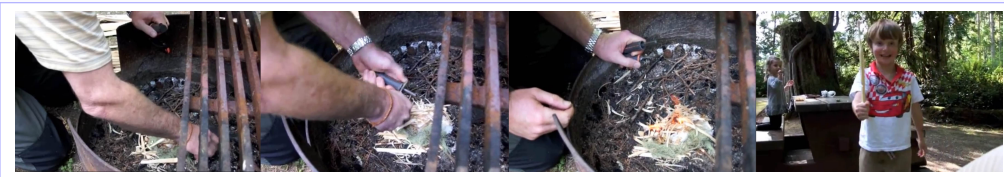


Figure 8: **Qwen3-VL-8B cyclic versus full-permutation Coverage curves.** The full-permutation design averages over all order contexts for each target position.

## Example 1.



### Position 1

A man demonstrates how to start a fire in a campground fire pit using a ✓ fire starter. He strikes the rod several times over a pile of tinder, which includes wood shavings and lichen, creating sparks. After a few tries, the tinder ✓ catches fire, and he successfully starts a small flame while his ✓ children watch.

### Position 2

A man at a campsite is preparing to start a fire inside a metal fire ring. He uses a ✓ fire striker to create sparks on a tinder bundle made of wood shavings and some white material. After a few tries, the tinder ✓ catches fire, and he successfully starts a small flame.

### Position 3

A man demonstrates how to start a campfire using a ✓ fire starter in a metal fire pit. He scrapes a ferro rod over a tinder bundle of wood shavings and lichen, creating sparks to ignite it. After a few strikes, ✓ the sparks catch, and he successfully starts a small flame.

### Position 4

A man at a campsite demonstrates how to start a fire using a ✓ ferro rod and tinder. He carefully arranges wood shavings and other flammable materials in a fire pit before striking the rod to create sparks. After a few tries, the sparks successfully ignite the tinder, and ✓ a small flame begins to grow.

Figure 9: **Example 1.** The four responses consistently preserve the core ignition-related details (e.g., *fire starter* and *catches fire*), while the contextual detail about children watching appears only in Position 1.

### Prompt-placement leakage example.

**Claimed target slot:** Position 4, “Drinking coffee”



**Source slot whose details leak in:** Position 1, “Having an ice cream”



**Target reference.** A big green garbage can is pushed up against a brick wall and a reindeer jumps out drinking from a coffee cup. The reindeer continues to drink out of the coffee cup and eventually falls out of over the garbage can.

**Source reference.** A little boy is filling an ice cream cone with ice cream. He licks the ice cream cone. He lifts the ice cream cone up to show the camera.

**Code-mined other-specific anchors.** cone; cream; ice; ice cream cone; enjoy cream; ice cream; capture with cream.

**Original model summary for the claimed target slot.** An animated deer climbs out of a green dumpster, holding an **ice cream cone** with excitement. The background features a brick wall and a street scene, adding context to the urban setting. The deer attempts to **enjoy its ice cream**, even managing to catch some of it in its mouth playfully. The scene is whimsical, capturing the deer’s joyful interaction with the **ice cream**.

**Human label.** Confirmed cross-video leakage: the claimed target video shows a deer/reindeer drinking from a cup, while the highlighted ice-cream anchors are supported by another video in the same input group.

Figure 10: **Manually verified prompt-placement leakage case.** The automatic miner selected the highlighted concrete anchors because they are unsupported by the claimed target reference but supported by another video in the same input group. The human audit labels this case as confirmed cross-video leakage.